

CHAPTER 147

Wave Overtopping and Sediment Transport over Dunes

Mark W. Hancock¹ and Nobuhisa Kobayashi, M. ASCE²

Abstract

Experiments were conducted on a sand beach to represent occurrences of minor to major dune overtopping by varying the spectral peak period of incident irregular waves. Both water overtopping and sand overwash rates were measured. The experimental results were compared to existing empirical formulas for equilibrium beach slopes (Kriebel, Kraus, and Larson, 1991), cross-shore sediment transport (Kraus and Mason, 1993), and irregular wave reflection (Seelig, 1983) from sand beaches. Scale and non-equilibrium effects were found to be important causes of discrepancies between predicted and measured values. Additionally, an empirical formula for the overtopping of coastal structures (De Waal and Van der Meer, 1992) was compared with overtopping measurements for the experimental dune. The empirical formula of De Waal and Van der Meer gave order-of-magnitude estimates, but could not account for the effects of the profile evolution within each test. The measured average volumetric sediment concentration was found to be independent of the normalized overtopping rate and varied by only a factor of two.

Introduction

Wave overtopping of dunes and barrier islands has been investigated in the past using site-specific field data (e.g., Holland *et al.*, 1991). However, the quantitative understanding of the overwash process remains rudimentary, partly because of the difficulties associated with field measurements during storms. At present, there is no predictive method to generalize the findings of site-specific field data. A knowledge of the overwash process is necessary for establishing a realistic boundary condition for existing beach and dune erosion models. For example, the simple empirical model of Kriebel (1990) simulates only offshore transport at the crest of the remnant dune and does not simulate the landward transport of sand due to overwash. The latest version of the storm-induced beach erosion model SBEACH (Wise and Kraus, 1993) allows for the landward transport of sand due to dune overwash, but prediction is based on simple geometric arguments related to the runup exceedance of the dune and the transport magnitude at the landward

¹Frederic R. Harris, Inc., 300 East 42nd St., New York, NY 10017

²Center for Applied Coastal Research, Department of Civil Engineering, University of Delaware, Newark, DE 19716

boundary of the surf zone.

Experimental Setup and Procedures

The experiment to collect data on the overwash of a subaerial dune was conducted in the tow tank located in the basement of DuPont Hall at the University of Delaware and is detailed in Hancock (1994). The tow tank is 30 m long, 2.44 m wide and 1.5 m deep. Figure 1 shows the tank layout. Irregular waves were generated using a piston-type wave paddle. A gravel beach was located 25 m away from the paddle to absorb waves and reduce the effects of re-reflection from the paddle. A 9.7 m long divider wall was constructed 0.61 m from one of the tow tank side walls. The dune overwash experiment was conducted in the 0.61 m wide flume. Figure 2 shows a detail of the experimental setup, including wave gage placement, at the beginning of each test, where d_t = water depth below still water level (SWL) at gage 1; d_s = water depth below SWL at the toe of the dune; H_c = positive crest height of the subaerial dune above SWL; m = slope of the seaward dune face; d_p = water depth of the horizontal bottom in front of the wave paddle; and B_c = horizontal distance between the dune crest and the seaward edge of the basin used to collect the overtopped water and overwashed sand. The height of the collection basin was 53 cm and was less than $(d_p + H_c)$. The initial beach profile was limited to a 1:23.5 slope, corresponding to the fixed beach tests on irregular wave overtopping over a 1:2 smooth revetment conducted by Poff and Kobayashi (1993a).

Five moveable bed tests for spectral peak periods, T_p , of 1.2, 1.4, 1.6, 1.8, and 2.0 seconds were conducted to represent occurrences of minor to major dune overwash. These tests will herein be referred to as tests MH1, MH2, MH3, MH4, and MH5 to distinguish them from further tests which will be conducted using the same facilities and procedures. Each test consisted of a series of runs, where each run duration was 325 seconds. A test was terminated when it appeared that further runs would expose the collection basin wall directly to wave action. Data

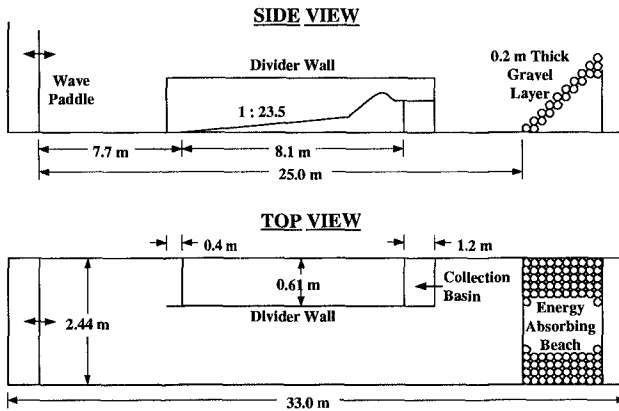


Figure 1: Layout of the Tow Tank

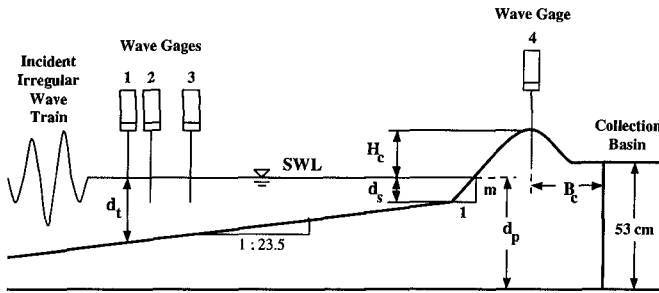


Figure 2: Experimental Setup

from the four wave gages were recorded during every test run. At the end of each test run, the volumes of overtopped water and overwashed sand in the collection basin were measured. The total volume of water collected was found by adding the volume of water pumped out of the collection basin to the volume of water held in the pores of the overwashed sand. The overtopping rate, \bar{Q}_w , and overwash rate, \bar{Q}_s , were determined by dividing the total volume of water and the volume of sand (no voids), respectively, by the test duration and flume width.

Beach and dune profiles were taken before each test and after runs of noticeable profile change. Three cross sections along the beach were profiled. One profile was taken at a distance of 20 cm from the plywood wall, another along the center line, and the last 20 cm from the tow tank wall. The average of these three profiles was calculated and this average profile was assumed to be uniform across the flume. The initial profile of a test was taken over the entire length of the beach at intervals of 10 cm. After runs of interest, profiles were taken from the seaward edge of the collection basin to a point of no net sediment transport, which was approximately 250 cm from the basin edge. Depths were sampled at an interval of 1 cm in order to distinguish smaller bed features such as ripples created by the wave action. The cross-shore variation of the net sediment transport rate, \bar{q}_s , for each test run was calculated using the continuity equation of sediment and the measured profiles starting from the seaward location of no profile change. The value of \bar{q}_s at the landward boundary corresponds to the net sediment transport rate into the collection basin and should be equal to the average overwash rate \bar{Q}_s for the same duration calculated from the collected sand.

The sand used in this experiment was well-sorted with a median diameter, d_{50} , of 0.38 mm. The measured value for the specific gravity, s , was 2.66, which falls within the expected range for quartz sand. The measured value for sediment proposity, n_p , was 0.41, which is reasonable for beach sand. The fall velocity, w , of the sediment was measured to be 5.29 cm/sec.

The parameters specified to the wave generation program (Poff and Kobayashi, 1993b), which accounts for the effect of directional random wave refraction, were d_p = water depth below SWL at the wave maker; d_t = water depth below SWL at gage 1; $(H_{mo})_p$ = spectral estimate of the significant wave height at the water depth d_p ; T_p = spectral peak period at the water depth d_p ; γ = peak enhancement

factor of the TMA spectrum at the water depth d_p ; s_{max} = maximum value of the directional spreading parameter at the water depth d_p ; α = predominant incident wave direction at the water depth d_p ; and m_t = bottom slope at the water depth d_t . The input parameters used for each test are shown in Table 1.

Table 1: Wave Generation Input Parameters

<i>Test</i>	MH1	MH2	MH3	MH4	MH5
T_p (sec)	1.2	1.4	1.6	1.8	2.0
d_p (cm)	46.5	46.5	46.5	46	45.5
d_t (cm)	44.3	43.4	44.8	43.7	43.2
$(H_{mo})_p$ (cm)	12.5				
γ	3.3				
s_{max}	10.0				
α (deg)	0.0				
m_t	1/23.5				

The initial dune profile geometry for each test was held as nearly constant as possible. However, some variability occurred due to the difficulties of manipulating significant quantities of sand. The still water level in each test was determined by matching the initial dune crest elevations of all the tests. The dimensions of the initial dune profiles for each test are given in Table 2 and are defined in Figure 2.

Table 2: Initial Dune Profile Geometry

<i>Test</i>	MH1	MH2	MH3	MH4	MH5
d_s (cm)	19.0	18.5	20.0	18.5	18.0
H_c (cm)	12.9	12.3	12.5	12.5	12.3
m	3.32	3.32	3.27	3.45	3.26
B_c (cm)	40.0				

Experimental Results

The measured time series and spectra of the incident and reflected waves varied very little from one test run to another. This implies that the incident and reflected waves were almost unaffected by the beach profile changes during each test. The mean of the measured spectral estimates of the significant wave height was 12.47 cm, which is nearly identical to the H_{mo} value of 12.5 cm specified to the wavemaker. The standard deviation of the measured H_{mo} values was 0.26 cm. The spectral peakedness parameter, Q_p , decreased with increased spectral peak period, T_p . Q_p ranged from a mean value of 5.4 in test MH1 with $T_p = 1.2$ sec, to

a mean value of 3.1 in test MH5 with $T_p = 2.0$ sec. Similarly, the spectral correlated parameter, κ , decreased with increased T_p , with a high mean value of 0.64 for test MH1 and a low mean value of 0.41 for test MH5. The average run length, \bar{j} , remained relatively constant throughout the experiment, with $1.30 \leq \bar{j} \leq 1.87$.

In general, the reflection coefficient, \bar{r} , tended to increase slightly with increasing spectral peak period. Within each test, the trend was that the measured value for \bar{r} decreased as the overtopping rate, \bar{Q} , increased. The values of \bar{r} ranged from 0.195 to 0.305. The values of \bar{Q} approximately doubled from test to test as T_p was increased by 0.2 sec. In each test, \bar{Q} increased during the initial runs before becoming a nearly constant value for the remainder of the runs, as can be seen in Figures 3 and 4. The normalized overtopping rates, $\bar{Q}/(H_s\sqrt{gH_s})$ with $H_s =$ significant wave height, ranged from 0.0 in run 1 of test MH1 to 0.00625 in run 4 of test MH5. Unlike the average overtopping rate, the measured average overwash rate trend varied significantly between tests. In test MH1, \bar{Q}_s increased during the initial runs before assuming a constant value over the final runs, as shown in Figure 3. Test MH2 displayed a similar trend in the initial runs, but after obtaining a peak value in run 3, \bar{Q}_s decreased appreciably before maintaining a nearly steady value. In tests MH3, MH4, and MH5, the value of \bar{Q}_s was relatively high in the first run, peaked in the second run, and then decreased with each remaining run. This trend is shown in Figure 4. The measured values of $\bar{Q}_s/(wd_{50})$ ranged from 0.0 in run 1 of test MH1 to 1.82 in run 2 of test MH5. The qualitative and quantitative trends of the average sediment concentration in volume were similar for each test. The calculated values for \bar{Q}_s/\bar{Q} tended to decrease as each test progressed, with the exception of test MH1, and ranged from 0.023 to 0.056.

The parameters used to describe the dune profile evolution were selected following the examples of the equilibrium beach profile presented by Kriebel, Kraus, and Larson (1991) and the equivalent slope for a coastal structure with a berm presented by De Waal and Van der Meer (1992). Many of the profile parameters

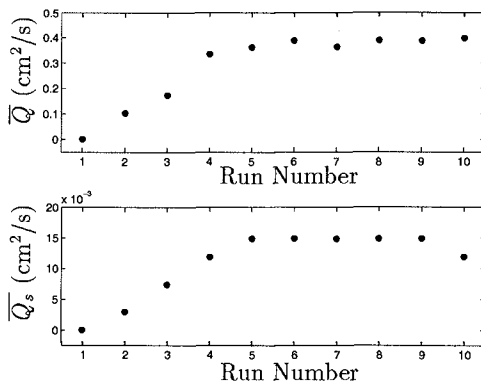


Figure 3: Overtopping Rate, \bar{Q} , (Top) and Overwash Rate, \bar{Q}_s , (Bottom) for MH1 with $T_p = 1.2$ sec.

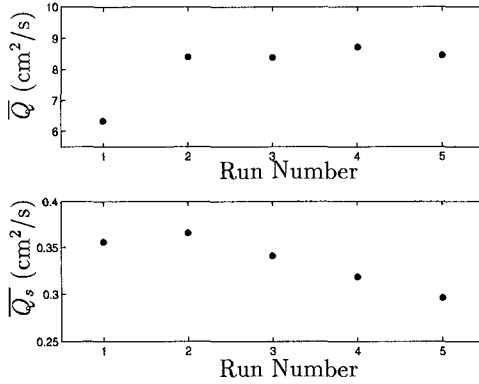


Figure 4: Overtopping Rate, \bar{Q} , (Top) and Overwash Rate, \bar{Q}_s , (Bottom) for MH5 with $T_p = 2.0$ sec.

are defined in Figure 5 where x = positive-seaward horizontal coordinate with an origin where the still water level (SWL) intersects the beach; d_s = depth relative to SWL below which there is effectively no profile change; H_s = depth below SWL equal to the average significant wave height between two measured profiles; B_s = horizontal distance from the dune crest to the depth H_s ; h = depth below SWL at a distance x seaward of the origin of the horizontal coordinate; H_c = dune crest height above SWL; m = fitted slope of the dune face from the crest to a point slightly below SWL; and B_c = horizontal distance from the dune crest to the edge of the collection basin. The concept of an equilibrium profile of the form $h = Ax^{2/3}$ was introduced by Bruun (1954), where h is the depth at a distance x offshore from the still water shoreline and A is the profile scale factor. For this analysis, A was found by fitting the two-thirds power profile to each measured profile. An additional parameter examined was the equivalent beach slope for wave runup and overtopping, m_e , expressed as

$$m_e = \frac{H_s + H_c}{B_s} \quad (1)$$

The dune profile evolutions for tests MH1 and MH5 are shown in Figures 6 and 7. For all of the test runs, d_s was greater than H_s , probably because these tests corresponded to a high dune and a large storm surge. Also, the crest height was always greater than $(53 - d_p)$ cm, which is the height of the collection basin above SWL. In each test, the fitted dune face slope and equivalent beach slope decreased as the profiles evolved. The range of m was 0.23-0.31 and the range of m_e was 0.11-0.30. The measured B_s values increased as the toe of the evolving beach advanced seaward and B_c went to zero. The initial value for B_s was about 84 cm in each test and the final values ranged from 173 cm in test MH1 to 119 cm in test MH5. In general, the steep dune was transformed to a more gentle beach by the waves. The fitted values of A ranged from 0.9 to 1.2 cm^{1/3} and decreased slightly as the tests with shorter spectral peak periods, and correspondingly longer durations, progressed. Kriebel, Kraus, and Larson *et al.* (1991) used field data

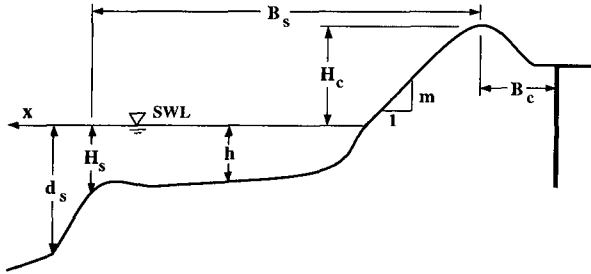


Figure 5: Definition Sketch for Profile Parameters

to obtain the following equation for the equilibrium value of A :

$$A \approx 2.25 \left(\frac{w^2}{g} \right)^{1/3} \tag{2}$$

where w is the sediment fall velocity and g is gravitational acceleration. Equation 2 is applicable for a water temperature of approximately 20° C and $1 \leq w \leq 10$ cm/sec. The measured w of the sand used in this experiment was 5.29 cm/sec, which yields $A = 0.69 \text{ cm}^{1/3}$ for an equilibrium profile. This A value is significantly less than the fitted $A = 0.9\text{-}1.2 \text{ cm}^{1/3}$ values, probably because the measured profiles were not in equilibrium and the experiment was a small-scale test.

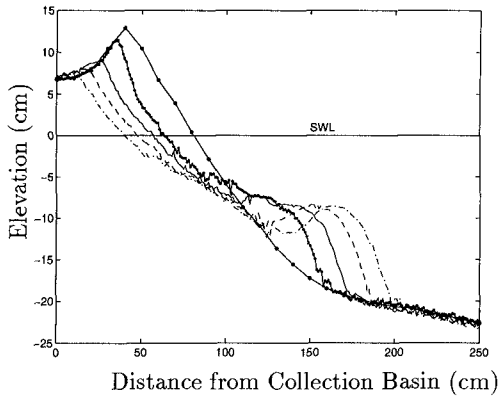


Figure 6: Dune Profile Evolution with Initial Profile (—●—) and Profiles after Run 1 (---), Run 3 (—), Run 6 (---), and Run 10 (-.-) for MH1 with $T_p = 1.2$ sec.

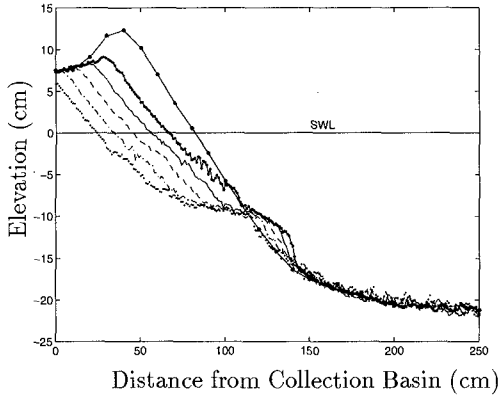


Figure 7: Dune Profile Evolution with Initial Profile (—●—) and Profiles after Run 1 (---), Run 2 (—), Run 3 (---), Run 4 (-.-), and Run 5 (···) for MH5 with $T_p = 2.0$ sec.

The calculated net cross-shore sediment transport rates, \bar{q}_s , which is positive onshore, as a function of the distance from the collection basin for run 1 of tests MH1, MH3, and MH5 are shown in Figure 8. It is apparent from the figure that there was an appreciable seaward transport of sand at the base of the dune during the first run of each test. The magnitude of this seaward transport decreased with increased T_p . The landward transport of sand observable at the dune crest was increased in the tests with larger T_p . In all of the tests, the amplitude of

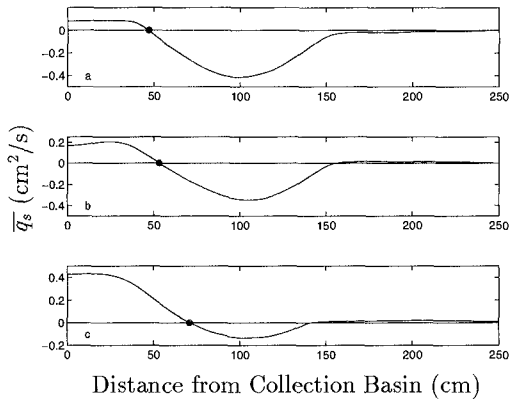


Figure 8: Average Cross-Shore Sediment Transport Rates During the First Run of a) Test MH1, b) Test MH3, and c) Test MH5.

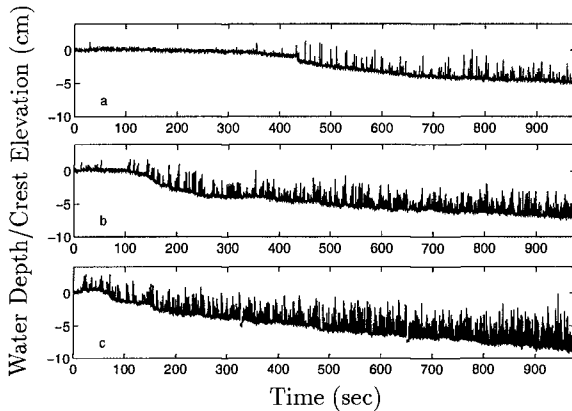


Figure 9: Gage 4 Time Series for a) Test MH1, b) Test MH2, and c) Test MH3.

\bar{q}_s between two measured profiles was appreciably smaller after the initial run. The landward transport of sand dominated after the initial run in tests MH4 and MH5.

The time series recorded by gage 4 for the first three runs of tests MH1, MH3, and MH5 are shown in Figure 9. During these early runs, it is easy to distinguish a defined baseline between overtopping events. This baseline corresponds to the time-dependent dune crest elevation relative to the initial dune elevation. In test MH1, essentially no overtopping occurred during the first 400 sec of the test. This period of limited overtopping is shorter in test MH3 and non-existent in test MH5. Once large overtopping events occurred on a regular basis, the sand elevation at gage 4 began to decrease approximately linearly with time. The location of the baseline at the end of three runs in each test demonstrates the increased erosion at the location of gage 4 as T_p increased.

Analyses of Experimental Results

Beach Slope

Kriebel, Kraus, and Larson (1991) reanalyzed the field data of Sunamura (1984) in terms of the sediment fall velocity, w , and proposed the following expression for the equilibrium foreshore slope, m :

$$m = 0.15 \left(\frac{wT}{H} \right)^{1/2} \quad (3)$$

Kriebel (1990) suggested that the root-mean-square wave height, H_{rms} , at breaking be used for H in Equation 3 since Sunamura did not specify this quantity for random waves. For the present analysis, the wave period T was taken to be the significant wave period, T_s .

Although the measured slopes tended to decrease as each test progressed, as already discussed, the empirical m values determined using Equation 3 remained nearly constant, with $0.13 \leq m \leq 0.15$, and significantly underpredicted the beach slope. Kriebel, Kraus, and Larson (1991) remarked that their analysis of field data

gave much smaller beach slopes for given $H/(wT)$ than those observed during the small-scale tests of Dalrymple and Thompson (1976). Additionally, the empirical m values are based on an equilibrium profile. Neither the stage of the profile evolution nor memory effects can be incorporated in the parameter $(wT_s)/H_{rms}$. Therefore, the empirical formula presented by Kriebel, Kraus, and Larson (1991) is too simplistic to incorporate the scale and non-equilibrium profile effects of the beach evolution in this experiment.

Cross-Shore Sediment Transport

Using field data, Kraus and Mason (1993) extended the profile parameter, \mathbf{P}_s , developed by Dalrymple (1992) to irregular waves:

$$\mathbf{P}_s = \frac{gH_{os}^2}{w^3T_p} = 26,500 \quad (4)$$

where H_{os} is the deep-water significant wave height and T_p is the spectral peak period. Offshore sediment transport was observed to occur for \mathbf{P}_s values significantly greater than 26,500.

The values of \mathbf{P}_s measured in the present experiment ranged from a high average value of 939 in test MH1 to a low average value of 553 in Test MH5. Because \mathbf{P}_s is inversely proportional to the spectral peak wave period, the onshore transport of sediment is expected to increase as T_p increases. This prediction is proven correct by Figure 8. All of the calculated \mathbf{P}_s were much less than the threshold value of $\mathbf{P}_s = 26,500$ determined by Kraus and Mason. This would seem to indicate exclusively onshore transport of sand in this experiment. However, both onshore and offshore sediment transport are observable in Figure 8. In particular, significant bar formation occurred in test MH1 as evidenced in Figure 6. It is uncertain whether overwash occurred in the field measurements of Kraus and Mason, but it is expected that overwash would act to increase the landward transport of sand. Equation 4 does not include the slope effect on the direction of net sediment transport. Therefore, the probable reasons that offshore sediment transport occurred despite the small \mathbf{P}_s values are that this experiment was a small-scale test and that the initial foreshore slopes were rather steep.

Irregular Wave Reflection

Seelig (1983) proposed that the average reflection coefficient, \bar{r} , for irregular waves could be expressed as

$$\bar{r} = \frac{\alpha\xi_p^2}{\xi_p^2 + \beta} \quad (5)$$

where ξ_p is the irregular wave surf similarity parameter defined as

$$\xi_p = \frac{m_i}{\sqrt{\frac{2\pi H_s}{gT_p^2}}} \quad (6)$$

with beach slope m_i at the still water intercept, significant wave height H_s , and spectral peak period T_p . Seelig recommended that for smooth slopes $\alpha = 1.0$ and $\beta = 5.5$.

Figure 10 is a plot of the measured reflection coefficients of each test versus the irregular wave surf similarity parameter values found from the measured T_p and

H_s . Three lines corresponding to $\alpha = 0.65$, $\alpha = 0.85$, and $\alpha = 1.05$ in Equation 5 are plotted in the top portion for comparison. Using $\alpha = 1.0$ appears to be a reasonable value to conservatively estimate \bar{r} . The bottom portion of Figure 10 shows a linear least-squares fit of the data. The formula for this fit is

$$\bar{r} = 0.106 \xi_p + 0.075 \quad \text{for } 1.10 \leq \xi_p \leq 2.01 \quad (7)$$

The data points display low scatter, with a standard deviation of 0.03.

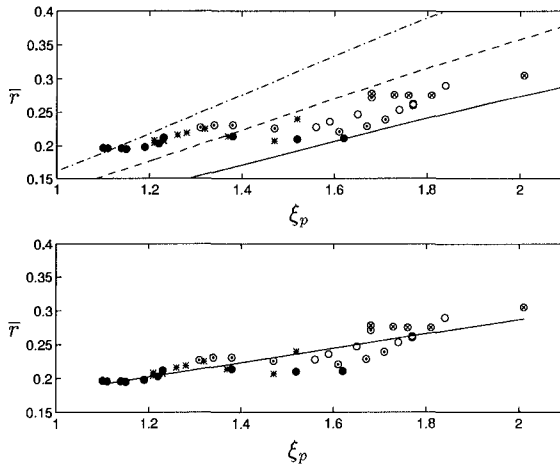


Figure 10: Reflection Coefficient, \bar{r} , versus Irregular Wave Surf Similarity Parameter, ξ_p , for Tests MH1 (\bullet), MH2 ($*$), MH3 (\odot), MH4 (\square), and MH5 (\otimes). Top Plot includes the Empirical Formula of Seelig (1983) for $\alpha = 0.65$ (—), $\alpha = 0.85$ (---), and $\alpha = 1.05$ (-·-). Bottom Plot includes Least-Squares Data Fit (—).

Irregular Wave Overtopping

The empirical formulas of De Waal and Van der Meer (1992) for the prediction of irregular wave runup and overtopping on coastal structures were compared to experimental results for dune overtopping. Since De Waal and Van der Meer did not have beach test data, their formulas are examined in the context of their applicability to the dune overtopping experiment. Their formula for predicting the 2%-runup, R_2 , which corresponds to the runup with an exceedance probability of 2%, is

$$\frac{R_2}{H_s} = 1.5 \gamma_f \gamma_h \gamma_\beta \xi_{p,eq} \leq 3.0 \gamma_f \gamma_h \gamma_\beta \quad (8)$$

where $\xi_{p,eq}$ is a breaking parameter based on an equivalent slope and modified by the influence factors γ_f for roughness effects, γ_h for shallow water effects, and γ_β for oblique wave attack effects. Since the present experiment involves only normally incident waves, $\gamma_\beta = 1.0$. Also, γ_f is assumed to be approximately 1.0 since a sand beach may be treated as a smooth slope.

The form of γ_h suggested by De Waal and Van der Meer, and modified here for application to dunes, is

$$\gamma_h = \begin{cases} 1 - 0.03 \left(4 - \frac{d_s}{H_s}\right)^2 & \text{for } 1 \leq \frac{d_s}{H_s} \leq 4 \\ 1 & \text{for } \frac{d_s}{H_s} \geq 4 \end{cases} \quad (9)$$

where d_s is the water depth at the toe of the dune as shown in Figure 5. They suggested an expression for $\xi_{p,eq}$ including berm effects, but for the present analysis it is assumed that $\xi_{p,eq} = \xi_e$, where

$$\xi_e = m_e T_p \sqrt{\frac{g}{2\pi H_s}} \quad (10)$$

with m_e = equivalent slope as defined in Equation 1. Equation 10 implies that wave runup is affected by the beach profile from the water depth H_s to the dune crest height, H_c , as shown in Figure 5. The simplified form of the normalized 2%-runup used in the dune analysis is, therefore,

$$\frac{R_2}{H_s} = 1.5 \gamma_h \xi_e \leq 3.0 \gamma_h \quad (11)$$

De Waal and Van der Meer proposed that the mean overtopping rate, \bar{Q} , was related to a "shortage in crest height", $R_* = (R_2 - H_c)/H_s$. By fitting about 500 data points from various overtopping tests, they came up with the following expression for the normalized overtopping rate, Q_* :

$$Q_* = \frac{\bar{Q}}{\sqrt{gH_s^3}} = 8 \times 10^{-5} \exp(3.1 R_*) \quad (12)$$

They observed a large data scatter, so that Equation 12 should be considered an order-of-magnitude estimate only.

The influence of the shallow water effects remained nearly constant throughout the present experiment with an average value of 0.82. However, the breaking parameter, ξ_e decreased as each test progressed and tended to increase with T_p , as is expected from Equation 10. The measured range of ξ_e was 0.48-1.77. The values of R_2/H_s and R_* followed the same qualitative trend as ξ_e , with $0.60 \leq R_2/H_s \leq 2.11$ and $-0.02 \leq R_* \leq 1.25$. The predicted decrease of R_2/H_s due to the decrease of m_e is greater than the measured decrease of the normalized crest height H_c/H_s . As a result, the predicted Q_* decreased as each test progressed and ranged from 0.7 to 38.7. However, as shown in Figures 3 and 4, the measured average overtopping rates increased in the early runs before becoming nearly constant. The equivalent slope, m_e , for dunes and coastal structures appears to be different in light of the opposite trend. A plot of the measured ($\ln Q_*$) versus R_* is shown in Figure 11. For comparison, Equation 12 is plotted in the top portion of Figure 11. It is apparent that the formula of De Waal and Van der Meer significantly underpredicts the dune overtopping rate in all but the first runs of the tests. However, the predicted values are within an order of magnitude of the measured results. A linear regression analysis of the data is shown in the bottom portion of Figure 11 and yields

$$Q_* = 3.35 \times 10^{-4} \exp(2.82 R_*) \quad \text{for } -0.02 \leq R_* \leq 1.25 \quad (13)$$

The slope of the fitted line is very close to that found from Equation 12 indicating a similar data trend, but the magnitude of Q_* found from Equation 13 is about four times greater. Bounding lines plotted for $(2.0 \times Q_*)$ and $(0.5 \times Q_*)$ show that there is a data scatter of a factor of about 2. Although the tests tend to fall along the fitted line, it is apparent that there are data trends within each test. Therefore, the stage of the dune profile evolution is an important factor that can not be accounted for in Equations 12 and 13.

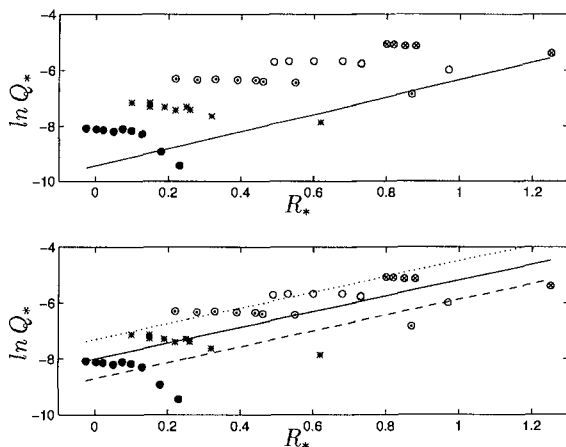


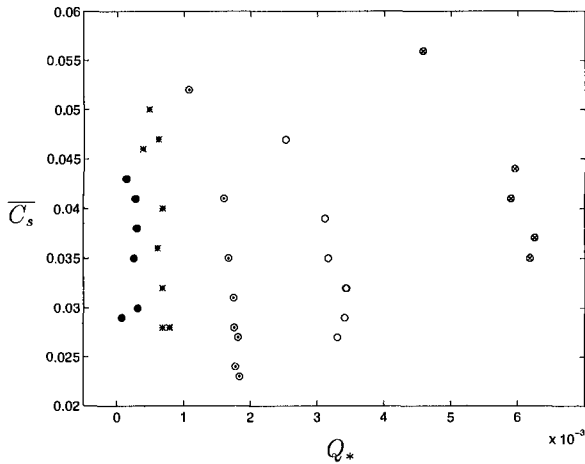
Figure 11: Natural Log of the Non-dimensional Overtopping Rate, Q_* , versus Non-dimensional 2% Runup Exceedance, R_* , of Tests MH1 (\bullet), MH2 ($*$), MH3 (\odot), MH4 (\circ), and MH5 (\otimes). Top Plot includes the Empirical Formula of De Waal and Van der Meer (1992) (—). The Bottom Plot includes a Least-Squares Data Fit $\ln(Q_*)$ (—), $\ln(2Q_*)$ (\cdots), and $\ln(0.5Q_*)$ ($---$).

Irregular Wave Overwash

The average volumetric sediment concentration, \overline{C}_s , is defined as

$$\overline{C}_s \equiv \frac{\overline{Q}_s}{\overline{Q}} \quad (14)$$

which is the ratio of the sediment (no voids) overwash rate, \overline{Q}_s , to the water overtopping rate, \overline{Q} . Figure 12 shows a plot of \overline{C}_s versus Q_* . It is apparent that no relationship exists between the two parameters in this experiment. The value of \overline{C}_s did tend to decrease as the profile evolved in all of the tests except test MH1. Nevertheless, the range of $\overline{C}_s = 0.023$ - 0.056 is surprisingly narrow in this experiment. Therefore, if \overline{C}_s remains approximately constant, \overline{Q}_s can be predicted for estimated \overline{Q} .



References

- Bruun, P. (1954). "Coast erosion and the development of beach profiles." Beach Erosion Board, Tech. Memo, No. 44.
- Dalrymple, R.A. (1992). "Prediction of storm/normal beach profiles." *J. Wtrwy. Port, Coast., and Oc. Engrg.*, ASCE, 118(2), 193-200.
- Dalrymple, R.A. and Thompson, W.W. (1976). "A study of equilibrium beach profiles." *Proc. 15th Coast. Engrg. Conf.*, ASCE, 1277-1296.
- De Waal, J.P. and Van der Meer, J.W. (1992). "Wave runup and overtopping on coastal structures." *Proc. 23rd Coast. Engrg. Conf.*, ASCE, 2, 1758-1771.
- Hancock, M.W. (1994). "Experiments on irregular wave overtopping and overwash of dunes." Thesis submitted for the degree of Master of Civil Engineering, Univ. of Delaware, Newark, DE.
- Holland, K.T., Holman, R.A., and Sallenger, A.H., Jr. (1991). "Estimation of overwash bore velocities using video techniques." *Coastal Sediments '91*, ASCE, 489-497.
- Kraus, N.C. and Mason, J.M. (1993). Discussion of "Prediction of storm/normal profiles." *J. Wtrwy. Port, Coast., and Oc. Engrg.*, ASCE, 119(4), 468-470.
- Kriebel, D.L. (1990). "Advances in numerical modeling of dune erosion." *Coastal Engineering*, 14, 2304-2317.
- Kriebel, D.L., Kraus, N.C., and Larson, M. (1991). "Engineering methods for predicting beach profile response." *Proc. Coastal Sediments '91*, ASCE, 557-571.
- Poff, M.T., and Kobayashi, N. (1993a). "Effects of toe depth and slope roughness on wave overtopping." *Proc. of the Hilton Head Intl. Coast. Symp.*, 1, 115-120.
- Poff, M.T., and Kobayashi, N. (1993b). "Computer program for refraction of directional random waves." *Res. Report No. CACR-93-04*, Ctr. for Appl. Coast. Res., Univ. of Delaware, Newark, DE.
- Seelig, W.N. (1983). "Wave reflection from coastal structures." *Proc. Coastal Struc. '83*, ASCE, 961-973.
- Sunamura, T. (1984). "Quantitative prediction of beach-face slopes." *Geol. Soc. of America Bulletin*, 95(2), 242-245.
- Wise, R.A. and Kraus, N.C. (1993). "Simulation of beach fill response to multiple storms, Ocean City, Maryland." *Proc. Coastal Zone '93, Coast. Beach Nourish. Engrg. and Mgmt. Considerations*, ASCE, 133-147.